

# Dielectric properties of epoxy/graphite flakes composites: Influence of loading and surface treatment

Slavica Maletić<sup>1</sup> | Nataša Jović Orsini<sup>2</sup> | Mirjana Milić<sup>2</sup> |  
Jablan Dojčilović<sup>1</sup> | Amelia Montone<sup>3</sup>

<sup>1</sup>Faculty of Physics, University of Belgrade, Belgrade, Serbia

<sup>2</sup>Department of Theoretical and Condensed Matter Physics (020), VINČA Institute of Nuclear Sciences – National Institute of the Republic of Serbia, University of Belgrade, Belgrade, Serbia

<sup>3</sup>Materials Technology Division, ENEA Centro Ricerche Casaccia, Roma, Italy

## Correspondence

Slavica Maletić, Faculty of Physics, University of Belgrade, Belgrade, Serbia.  
Email: [sslavica@ff.bg.ac.rs](mailto:sslavica@ff.bg.ac.rs)

Nataša Jović Orsini, Department of Theoretical and Condensed Matter Physics (020), University of Belgrade, P.O. Box 522, RS 11001 Belgrade, Serbia.  
Email: [natasaj@vin.bg.ac.rs](mailto:natasaj@vin.bg.ac.rs)

## Funding information

Ministarstvo Prosvete, Nauke i Tehnološkog Razvoja, Grant/Award Numbers: 451-03-47/2023-01/200017, 451-03-47/2023-01/200162

## Abstract

Epoxy-rich carbon-based composites are well recognized materials in industries owing to their good mechanical properties and thermal stability. Here, dielectric properties of composites based on bisphenol-A-epoxy resin loaded with 5, 6, 10, and 15 wt% of graphite flakes (GF) have been studied. The frequency and temperature dependence of the dielectric permittivity, dielectric loss, and *ac* conductivity have been examined in temperature (−103 to 97°C) and frequency (20 Hz–200 kHz) range. Influence of the filler surface chemistry have been studied for composites loaded with 5 wt% GF obtained: (i) under wet milling, without or with adding Triton-100x as a surfactant, or (ii) under dry milling in the presence of KOH. The composite made of epoxy loaded with 5 wt% exfoliated expanded graphite flakes (EEG), was also prepared. The surface treatment with KOH notably increased dielectric constant of the composite, keeping low dielectric loss, while treatment with Triton-100x significantly increased  $\tan\delta$ . The composite loaded with exfoliated expanded graphite shows higher *ac* conductivity than those obtained with flaky graphite, GF. Possibility to change dielectric properties of the composites without changing the loading content can be used as an approach in tailoring one with desired dielectric properties.

## KEYWORDS

composites, dielectric properties, functionalized surfaces, graphite nanosheets

## 1 | INTRODUCTION

Composites consisting of polymer matrix and various types of fillers have been extensively studied for a wide range of applications from microelectronic, optoelectronic, and energy harvesting system, to automotive and aerospace industry.<sup>1</sup> Application of composites depends on their performances, which are strongly related to the choice of polymer matrix and filler, the preparation and post-production routes, composite architecture, and so forth. Various materials have been tested as a filler, from

ceramics (TiO<sub>2</sub>, Al<sub>2</sub>O<sub>3</sub>, ZnO, BaTiO<sub>3</sub>, ...), metal compounds (boron nitride, aluminum nitride, copper, ...) to carbon-based nanostructures.

Electrically conductive composites with carbon-based fillers (such as carbon nanotubes, carbon black, graphene, or graphite flakes [GF]), attracted huge attention due to usually high electrical conductivity and good mechanical properties.<sup>2</sup> They can be interesting for extensive use in resistors (when beyond the critical concentration of filler the polymer becomes conductive).<sup>3</sup> Other applications of composites are directed toward

over-current and over-temperature circuit protection devices, super capacitors, biosensors,<sup>4</sup> antistatic materials and materials for electromagnetic interference (EMI) shielding.<sup>2,5-7</sup>

A variety of phenomena (such as a sharp drop of resistivity at some critical filler content, increase of dielectric permittivity with filler content increase), are characteristic for composites based on mixing insulating polymer matrix with electrically conducting fillers.<sup>8</sup> Dielectric properties of such composites reflect their ability to store and consume electrostatic energy in an alternating (AC) electric field, while the electric conductivity study refers to their ability to transport electric charges.

When a polymeric material is found in an external electric field, its response is governed by different *polarization mechanisms*. Generally, the polarization of any material comes from four different contributions: dipolar, atomic, electronic, and interfacial polarization.<sup>9</sup> In polymers with *dipole* groups, the mechanism of orientation of dipole side groups or dipole segments corresponds to *Debye's relaxation polarizations*.<sup>10</sup> The dipolar segmental relaxations or dipolar group relaxations correspond to  $\beta$ -relaxations. The most important mechanisms of  $\beta$ -relaxation are movement of dipole side groups about the C-C chain or a local motion of very short segment of the polymer (such as the twisting of the hydroxyl or carbonyl side groups).<sup>11-13</sup> Another type of relaxations, known as  $\gamma$ -relaxation, is related to faster relaxation processes that occur below glass transition temperature of matrix (e.g., movement of the diphenyl propane group, rotation of the methylene sequence or the hydroxyl-ether group, etc.). The  $\alpha$ -relaxations are those which occur close and above the glass transition temperature ( $T_g$ ) of composite, usually due to translation of the main polymer chain through the medium.<sup>13</sup>

Dielectric properties of composites are largely determined by the nature of the filler/matrix interface, the filler surface area and the inherent conductivity of the fillers. At low electric field frequencies, dominates so-called *interfacial* (or space charge) polarization due to accumulation of free charges at the interfaces between two phases (filler and matrix), which differ in electrical conductivity.<sup>11,14</sup> In such composites, the dielectric behavior is subjected to the Maxwell-Wagner (MW) interfacial polarization when one of the components has higher electrical conductivity, compared to the other one.<sup>11</sup> Above the percolation threshold,  $p_c$  (at which the insulating-conducting transition can be observed), the dielectric response of polymeric materials will be additionally influenced by *electron conduction process*.

Composite materials based on epoxy resin filled with graphene or GF, or their functionalized counterparts

(e.g., graphene/graphite doped with heteroatoms such as e.g., oxygen or nitrogen) have been widely investigated.<sup>5,8,15,16</sup> It is well known that the lateral size, the aspect ratio and shape of flakes used as fillers have strong impact on dielectric properties of composites.<sup>5,17</sup> For example, Corcione et al. studied the dielectric properties of epoxy-based composites loaded with different kind of graphite precursors (expanded graphite, commercial graphene nanoplatelets, natural graphite).<sup>18</sup> They revealed that the expanded graphite (EG) with the highest aspect ratio improved the electrical performance of composite the best. The conductivity of such composites can be increased by several orders of magnitude, as the content of expanded graphite increased up to a critical level of loading.<sup>19</sup> N. Chand et al., studied the frequency and temperature dependence of dielectric properties of composite based on epoxy resin and graphite.<sup>20</sup> They found a shift of  $\tan\delta$  peaks toward higher temperatures in composite loaded with 2.9 wt% GF and assigned it to the increase of dipole relaxation time. Further, significant improvements of the dielectric properties were obtained in composites made of at least three components.<sup>21</sup> Vovchenko et al., showed that the permittivity was substantially increased when in addition to GF, carbonyl iron was added into epoxy.<sup>22</sup> The new approaches in designing epoxy-based materials go toward 3D alignment of carbon-decorated nanofillers with improved composites performances (such as thermal conductivity, electrical conductivity, etc.).<sup>23</sup>

In order to improve the interfacial adhesion with the matrix various surface treatments of carbon-based fillers have been studied, such as, treatments with: UV/ozone,<sup>24</sup> organic compounds (e.g., isocyanates,<sup>25,26</sup> acids,<sup>27</sup> polypyrrole (PPy),<sup>28</sup> *p*-phenylenediamine<sup>29</sup>), polyoxometalate,<sup>30</sup> cationic or anionic surfactants, KOH,<sup>31,32</sup> and so forth. Orientation of fillers in a certain direction inside a matrix also plays a very important role for obtaining composites with particular dielectric performances.<sup>23,33</sup>

In this paper, dielectric properties of composites based on bisphenol-A-epoxy resin loaded with different content of GF (5, 6, 10, and 15 wt%) have been studied. GF were obtained upon prolonged milling of pure graphite. The frequency and temperature dependence of the dielectric permittivity ( $\epsilon_r$ ), dielectric loss ( $\tan\delta$ ), and *ac* conductivity ( $\sigma_{ac}$ ) have been examined in temperature ( $-103$ – $97^\circ\text{C}$ ) and frequency (20 Hz–200 kHz) range. Influence of the filler surface chemistry have been studied for composites loaded with 5 wt% GF, used as-prepared or functionalized with Triton-100x surfactant or KOH. In addition, dielectric properties of the composite made of epoxy loaded with 5 wt% exfoliated expanded graphite flakes (EEG), were also examined.

## 2 | MATERIALS AND METHODS

### 2.1 | Materials preparation

For the preparation of the composites, we used GF obtained upon prolonged milling of graphite powder (Aldrich, 99.9% pure) in a mortar grinder. During milling in a Pulverisette 2, Fritsch mortar grinder, the vertical pressure of a pestle was 10 daN and no lateral pressure was set up. Three grams of pure graphite were milled with 15 mL of deionized water for 20 h. Thus, obtained graphite flakes were labeled as GF. Then, the procedure was repeated but with addition of Triton-100x (3 mL) as a surfactant (GF-Tr100x). Further, 3 g of pure graphite were milled under dry condition (without water) in a Retsch Ultra-Fine mortar grinder (Type KM1), with 60 g of potassium hydroxide, KOH, for 10 h. Afterwards, the GF were extensively washed with water. This way obtained GF were labeled as GF-KOH.

The matrix used to adopt GF was epoxy resin based on bisphenol-A-(epichlorhydrin) (Struers). The composites were prepared following procedure: 6 mL of bisphenol-A-(epichlorhydrin) were added to the mixture of GF-flakes in alcohol, sonicated for 3 h (to ensure homogeneous dispersion) and dried at 60°C (to ensure evaporation of alcohol). Then, 1 mL of epoxy hardener, triethylenetetramine, was added, followed by careful stirring for 15 min. The mixture was cast into a flat glass mold and degassed under vacuum overnight at room temperature. Before the composites were taken out from the mold, they were post-cured at 127°C for 10 min in air. The composites with the following weight fractions of GF were prepared: 5, 6, 10, and 15 wt%, labeled as epoxy/GF5, epoxy/GF6, epoxy/GF10, and epoxy/GF15, respectively. Pure epoxy (without fillers), as well as composites loaded with 5 wt% of: GF-Tr100x, GF-KOH, and exfoliated EEG (obtained upon prolonged sonication of expanded graphite) were also made. The obtained composites have uniform thickness of about 1 mm.

### 2.2 | Characterization

Scanning electron microscopy (SEM, FEI, Scious 2 Dual-Beam) was used to observe the morphology of pristine graphite and GF, as well as the fracture surfaces of pure epoxy and composites. The fracture was obtained after exposure of composite/pure epoxy to liquid nitrogen. X-ray diffraction (XRD) patterns of hexagonal graphite powder and GF were collected on a Bruker D8 Advance diffractometer in a glaze angle incident geometry (2°) (30 mA, 38 kV). The XRD patterns of pure epoxy and

epoxy/graphite composites loaded with 5, 10, and 15 wt% GF flakes were collected on Rigaku SamrtLab diffractometer. The solid-state <sup>13</sup>C NMR (nuclear magnetic resonance) spectrum of GF graphite flakes was collected using a Bruker spectrometer with magic-angle spinning (MAS) at 5 kHz. Spectrum was collected with proton cross-polarization (CP-MAS) and with proton decoupling (DP-MAS). GF flakes and composites were also characterized with Fourier transform infrared spectroscopy (Thermo Scientific Nicolet iS50 device with attenuated total reflection [ATR-FTIR] measurement). The specific surface area,  $S_{\text{BET}}$ , of GF flakes was determined following the Brunauer–Emmett–Teller (BET) approach.

Dielectric spectroscopy measurements were carried out using Precision LCR instruments (Hameg 8118), over a frequency range from 20 Hz to 200 kHz and a temperature interval from −103 to 97°C. Data acquisition was performed in the heating mode, with the heating rate of 2 °C/min. The temperature was recorded using a temperature controller (Lake Shore 340). The applied voltage was 1.5 V. A sample was placed in a closed capacitor cell with cell electrodes 13 mm in diameter, under vacuum ( $10^{-4}$  Pa), avoiding use of any paste. Acquisition of the conductance ( $G_{\text{m}}$ ) and susceptance ( $B_{\text{m}}$ ) of a sample, as well as, the conductance ( $G_{\text{b}}$ ) and susceptance ( $B_{\text{b}}$ ) of an empty cell with space between electrodes equal to the thickness of the sample, for the same test frequency and at the same temperatures, was carried out with specially programmed software. Details about the experimental setup can be found in the literature.<sup>34–36</sup>

*Specific conductance (G)* and *specific susceptance (B)* was calculated according to the equations:

$$G = (G_{\text{m}} - G_{\text{b}}) \cdot d/S \quad (1)$$

$$B = B_{\text{m}} - (B_{\text{b}} - 2\pi f \epsilon_0 S/d) \quad (2)$$

where  $d$  is the spacing between electrodes and  $S$  is the area of the electrode. Then, the *dielectric loss* ( $\tan\delta$ ) and *dielectric permittivity* ( $\epsilon_r$ ) were calculated as:

$$\tan\delta = G/B \quad (3)$$

$$\epsilon_r = Cd/\epsilon_0 S \quad (4)$$

where  $C = B/2\pi f$ , is the capacity,  $\epsilon_0$  is the vacuum permittivity ( $8.85 \times 10^{-12}$  F/m) and  $f$  is the frequency ( $\omega = 2\pi f$ , is the angular frequency) of the applied electric field.

The AC *conductivity* ( $\sigma_{\text{ac}}$ ) was evaluated from the values of dielectric data using a relation:

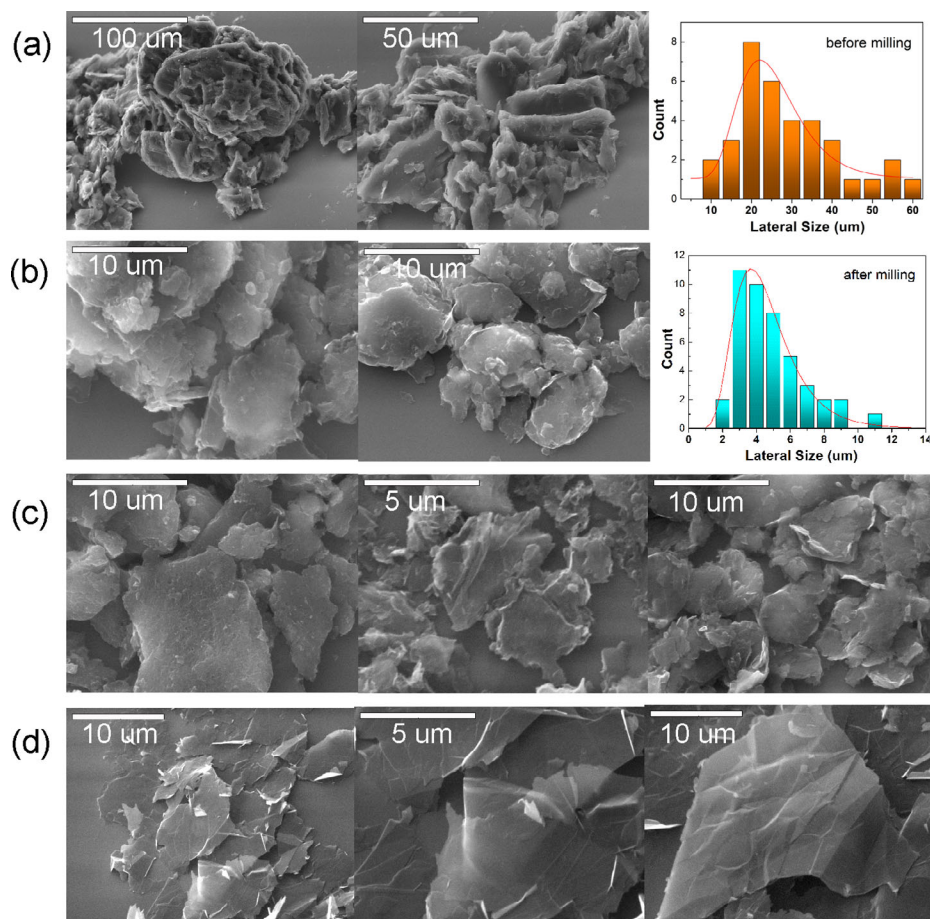


**FIGURE 1** Scanning electron microscopy photos of (a) pristine graphite and (b–d) fillers used to obtain epoxy-based composites: (b) graphite flakes (GF) obtained upon milling of pristine graphite in the presence of water without (GF, left) or with the presence of Triton-100x (GF-Tr100x, right); (c) GF obtained upon milling in the presence of KOH (GF-KOH); and (d) exfoliated EEG. [Color figure can be viewed at [wileyonlinelibrary.com](http://wileyonlinelibrary.com)]

$$\sigma_{ac} = \omega \varepsilon_0 \varepsilon_r \tan \delta. \quad (5)$$

## 3 | RESULTS AND DISCUSSION

### 3.1 | Structure and morphology

SEM photos of pristine graphite and fillers (GF, GF-Tr100x, GF-KOH, and EEG) used to obtain epoxy-based composites, are shown in Figure 1. It is obvious that the milling induces the lateral size decreasing. GF, with an lateral size in the range from 2 to 11  $\mu\text{m}$  (average in-plane size is about 4  $\mu\text{m}$ ; Figure 1b), were obtained under prolonged milling of pure graphite for 20 h. Presence of water as a lubricant, during a milling process seems to allow easier cleavage of graphite plates and give rise to less stress on  $\text{sp}^2$ -planes. On the contrary, dry milling in the presence of KOH powder induces roughness on the  $\text{sp}^2$ -surface of GF and produced (to some extent) graphite dust (see Figure 1c). SEM images confirmed that the EEG flakes has higher aspect ratio than GF flakes (Figure 1d).

XRD pattern of graphite powder, before and after milling, shown in Figure 2a, confirms a hexagonal crystal

structure. Noticeable decrease in the intensity of (002) reflection (inset of Figure 2a), point out on a dominant cleavage effect upon mechanical milling of 20 h. On the contrary, milling in the presence of KOH for 10 h produced thicker multi-layered structure of GF (inset of Figure 2a). No changes of the reflection positions were observed. Figure 2b shows the DP-MAS and (inset) CP-MAS spectra of GF graphite flakes. They are similar and show that the signal is coming from the solid-phase. The broad resonance at ca. 110 ppm in CP-MAS and at 124 ppm in DP-MAS spectra can be assigned to  $\text{sp}^2$ -hybridized carbon ( $-\text{C}=\text{C}-$ ) in the structural model of the aromatic domains. The reported value of chemical shifts (CS) for graphite plates, obtained upon milling, are close to the CS-values reported for graphene (117–132 nm<sup>37</sup>). The ATR-FTIR spectra of graphite flakes, GF, and GF-Tr100x (obtained after 20 h of millings under wet conditions without or with the presence of Triton-100x), and GF-KOH (obtained after 10 h of dry milling with KOH) are shown in Figure 2c. The ATR-FTIR spectrum of GF flakes, with a band at  $\sim 1224 \text{ cm}^{-1}$  assigned to bending of C–H groups, confirmed that the graphitic surface is almost free of functional groups. On the contrary, in the GF-Tr100x flakes presence of the functional groups

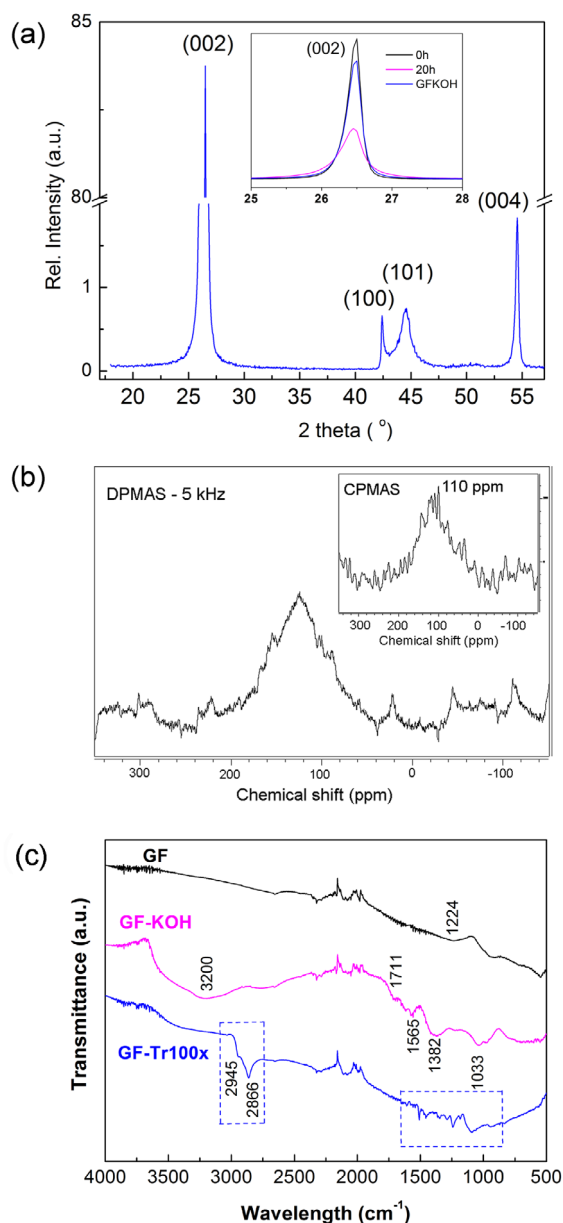


**FIGURE 2** (a) XRD diffraction pattern of hexagonal graphite powder (inset: the (002) reflection of graphite before and after milling for 20 h, and after milling for 10 h in the presence of KOH); (b)  $^{13}\text{C}$  solid-state DP-MAS and CP-MAS NMR spectra of GF flakes and (c) ATR-FTIR spectra of graphite plates obtained by milling under different conditions (GF, GF-Tr100x, and GF-KOH). [Color figure can be viewed at [wileyonlinelibrary.com](https://onlinelibrary.wiley.com/terms-and-conditions)]

coming from the surfactant Triton-100x is noticed by FTIR spectroscopy (bands framed by rectangles on Figure 2c). Thus, the band at  $\sim 2945\text{ cm}^{-1}$  can be assigned to the alkyl groups (C—H bonds that are in  $\text{sp}^3$  hybridization), while the band at  $\sim 2866\text{ cm}^{-1}$  comes from the stretching of the aliphatic C—H groups. Milling with KOH introduced the oxygen-containing groups on the basal plane of graphite flakes.<sup>38</sup> The band at  $\sim 1711\text{ cm}^{-1}$  can be assigned to C=O stretching vibration

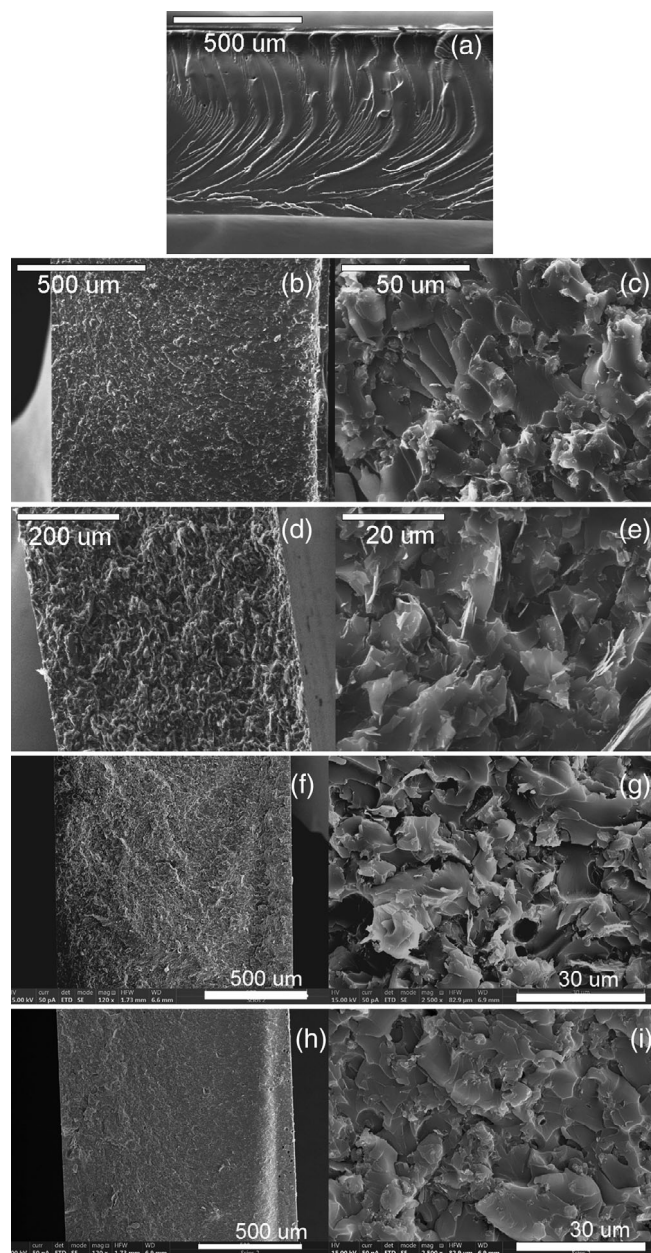


**FIGURE 3** Scanning electron microscopy images of fracture surfaces of (a) pure epoxy, (b, c) epoxy/GF5, (d, e) epoxy/EEG5, (f, g) epoxy/GF-Tr100x5, and (h, i) epoxy/GF-KOH5 composites (loaded with 5 wt% of graphite flakes).

in carboxylic acid and carbonyl moieties, the bend at  $\sim 1382\text{ cm}^{-1}$  can be assigned to stretching of C=O and bending of OH groups as a part of oxygen-containing functional groups, while the band at  $1033\text{ cm}^{-1}$  can be assigned to C—O—C in epoxy groups. A wide band between  $3000$  and  $3600\text{ cm}^{-1}$  represents the stretching vibrations due to the presence of hydroxyl group.

SEM micrographs of the fracture surfaces of pure epoxy, epoxy/GF5, epoxy/EEG5, epoxy/GF-Tr100x5, and epoxy/GF-KOH5 composites (loaded with 5 wt% of

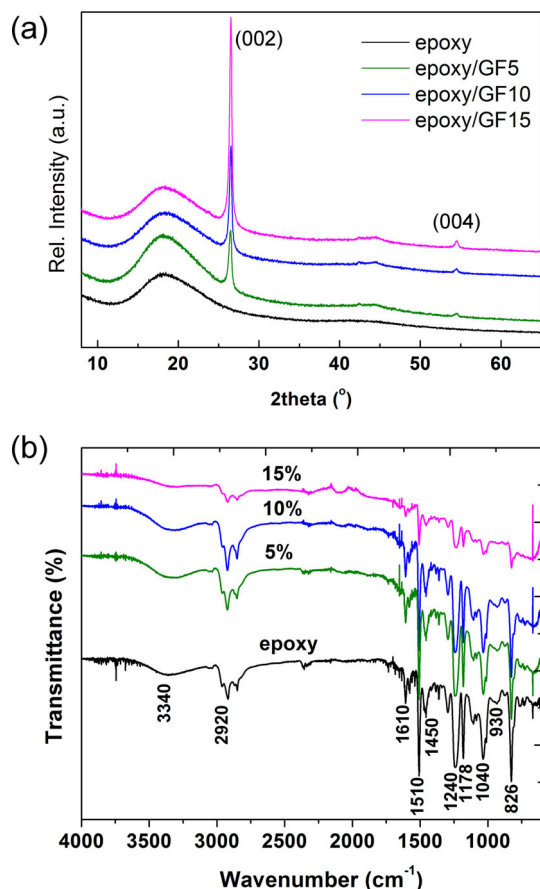


**FIGURE 4** (a) The XRD patterns of pure epoxy and epoxy/GF composites loaded with 5, 10, and 15 wt% of GF flakes; (b) the FTIR spectra of epoxy/GF5, epoxy/GF10, and epoxy/GF15 composites. [Color figure can be viewed at [wileyonlinelibrary.com](http://wileyonlinelibrary.com)]

graphite flakes), are shown in Figure 3a–i. Figure 3b revealed not fully uniform dispersion of GF graphite flakes across the section of composite, probably as a result of a partial sedimentation of fillers during composite hardening. On the contrary, well dispersed EEG and GF-Tr100x flakes within the epoxy matrix, cut into fragments with rough surfaces, are observed in the epoxy/EEG5 (Figure 3d,e) and the epoxy/GF-Tr100x5 (Figure 3f,g) composites, respectively (Figure 3d–i). It is worth to notice that the epoxy/GF-Tr100x5 composite was very hard to break, probably due to the adhering effect of Triton-100x surfactant, which helps in better networking of GF-Tr100x flakes with epoxy comparing to nonfunctionalized GF flakes. On the contrary, the fracture surface of epoxy/GF-KOH5 composites was observed with much lower contrast comparing to the epoxy/GF-Tr100x5 one, indicating the presence of thicker, multi-layered graphite layers. The graphite dust, observed in the GF-KOH filler seems to stay aggregated inside the epoxy/GF-KOH5 composite, giving characteristic shape of the fracture (Figure 3i).

Figure 4a shows the XRD patterns of pure epoxy and epoxy/GF composites loaded with 5, 10, and 15 wt% of GF flakes, while their FTIR spectra are shown in the Figure 4b. A broad peak with maximum at  $2\theta = 18^\circ$  coming from the epoxy, while the characteristic peaks of graphite, (002) and (004) at  $26.5^\circ$  and  $54.5^\circ$ , respectively, are well noticed, too. The FTIR spectra of composites show all the absorption bands characteristic for epoxy-based composites.

## 3.2 | Dielectric properties of the epoxy/GF composites

### 3.2.1 | Dielectric permittivity

The Figure 5a–d shows the temperature dependence of dielectric permittivity,  $\epsilon_r(T)$ , for pure epoxy matrix and composites loaded with 6, 10, and 15 wt% of graphite flakes (epoxy/GF6, epoxy/GF10, and epoxy/GF15), measured at different frequencies: 180 Hz, 800 Hz, 8 kHz, 18 kHz, and 80 kHz. The  $\epsilon_r$  value increases with temperature rise, independently of the frequency,  $f$ , in all samples, while with the frequency increase from 180 Hz to 80 kHz slight decrease of the  $\epsilon_r$  values was observed at all temperatures. The amount of loaded graphite flakes changes the dielectric permittivity value ( $\epsilon_r$ ) of composites the most. It is due to the increased number of micro-capacitors which are formed between conducting filler and epoxy layer and consequently, the increase of interfacial polarization between these two phases. The slight bend observed around  $27^\circ\text{C}$ , the most pronounced in pure epoxy, most likely corresponds to the  $\beta$ -dipolar group relaxations of epoxy molecule.<sup>39</sup> Except for the increase in the  $\epsilon_r$  value, no significant changes in  $\epsilon_r(T)$  function were observed for the pure epoxy resin and the epoxy/GF6 composite. Instead, in epoxy/GF10 and epoxy/GF15 composites (with higher loading content), more pronounced increase of dielectric permittivity is observed at temperatures higher than c.a.  $67^\circ\text{C}$ , at all frequencies. Since, the glass transition temperature,  $T_g$ , of pure epoxy is found at  $T_g \approx 75^\circ\text{C}$ ,<sup>19</sup> the softening of epoxy matrix at these temperatures is expected, possibly resulting in formation of direct contact between graphite flakes and, thus, the formation of conductive network.

Figure 6a shows the frequency dependence of the  $\epsilon_r$  value,  $\epsilon_r(f)$ , measured at  $T = 17^\circ\text{C}$ , for the epoxy/GF6, epoxy/GF10, and epoxy/GF15 composites. The increase of the  $\epsilon_r$  value with increasing the loading of graphite flakes in composites was observed in the frequency range from 30 Hz to 130 kHz. It is especially noticeable at lower electric field frequencies, when *interfacial* polarization

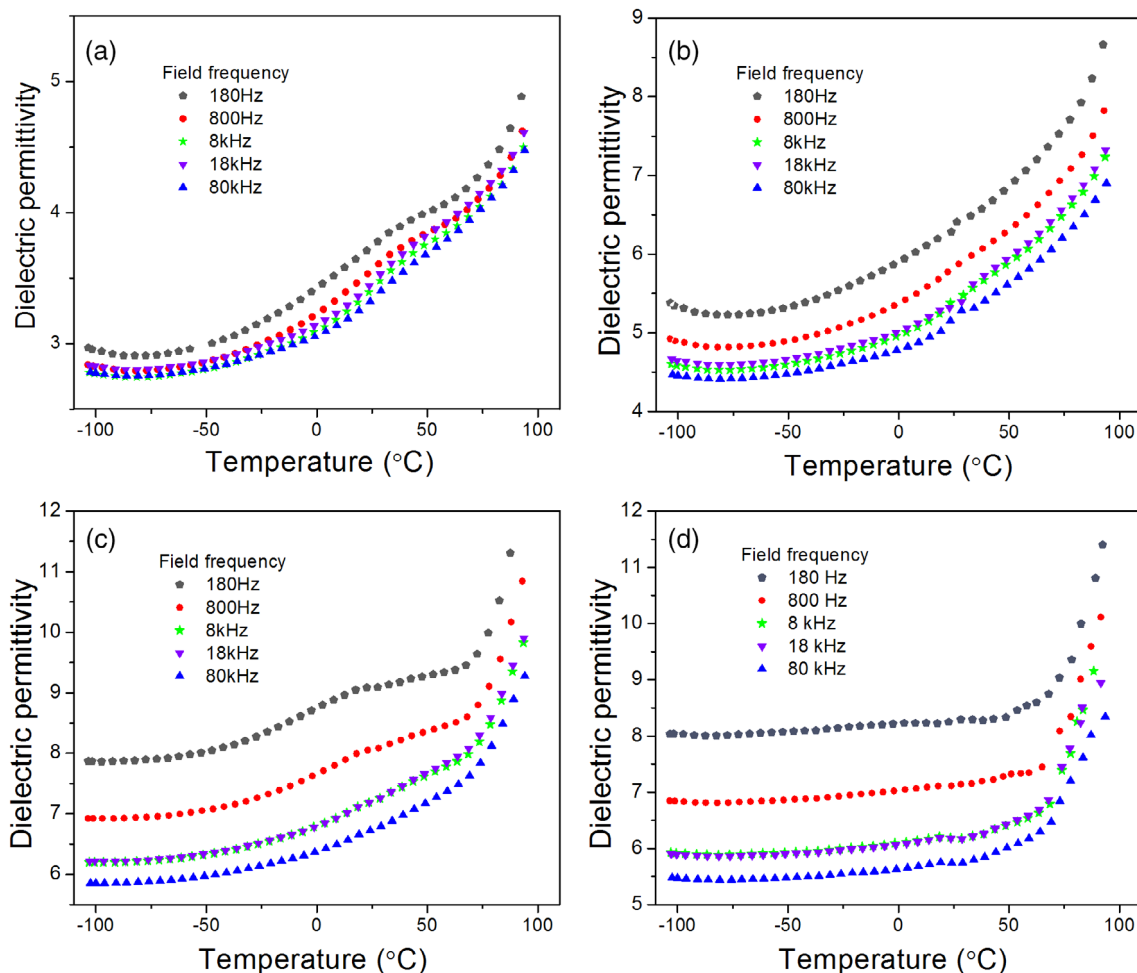


**FIGURE 5** Temperature dependence of dielectric permittivity for (a) pure epoxy, (b) epoxy/GF6, (c) epoxy/GF10, and (d) epoxy/GF15 composites, at different frequencies (180 Hz, 800 Hz, 8 kHz, 18 kHz, and 80 kHz). [Color figure can be viewed at [wileyonlinelibrary.com](http://wileyonlinelibrary.com)]

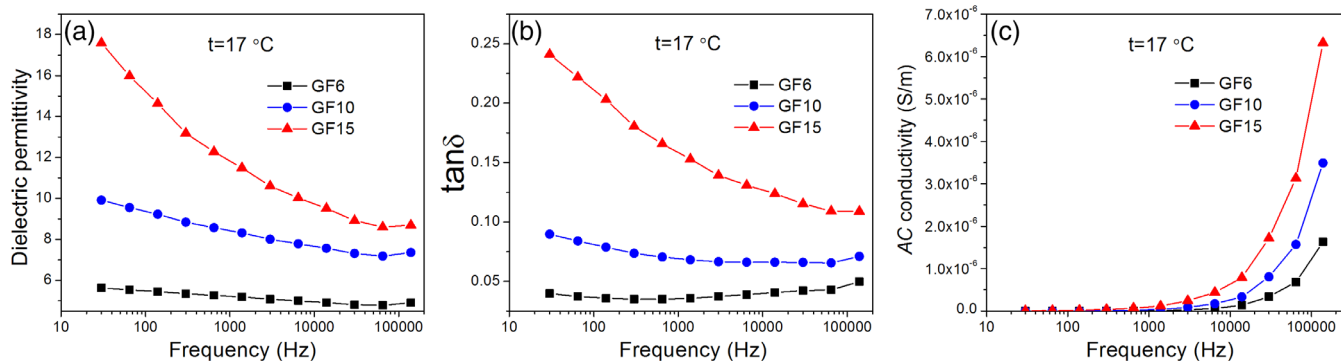


**FIGURE 6** Frequency dependence of (a) the dielectric permittivity,  $\epsilon_r$ , (b) the dielectric loss,  $\tan\delta$ , and (c) the ac conductivity,  $\sigma_{ac}$ , at temperature 290 K, for epoxy/GF6, epoxy/GF10, and epoxy/GF15 composites. [Color figure can be viewed at [wileyonlinelibrary.com](http://wileyonlinelibrary.com)]

dominates (accumulation of free charges at the interfaces between epoxy and graphite flakes).<sup>18,20</sup> At 30 Hz, the dielectric permittivity of the epoxy/GF15 composite is about three times higher than in the epoxy/GF6 composite (Figure 6a). These results once more point out that the number of formed micro-capacitors in composites

increases with increasing the filler loading. Thus, the local electric field, generated within composite due to the *interfacial* polarization, becomes stronger, resulting in the increase of the dielectric permittivity.<sup>6,11</sup> In addition, the  $\epsilon_r$  value decreases with increasing the applied field frequency, in all three composites. Decreasing is the most

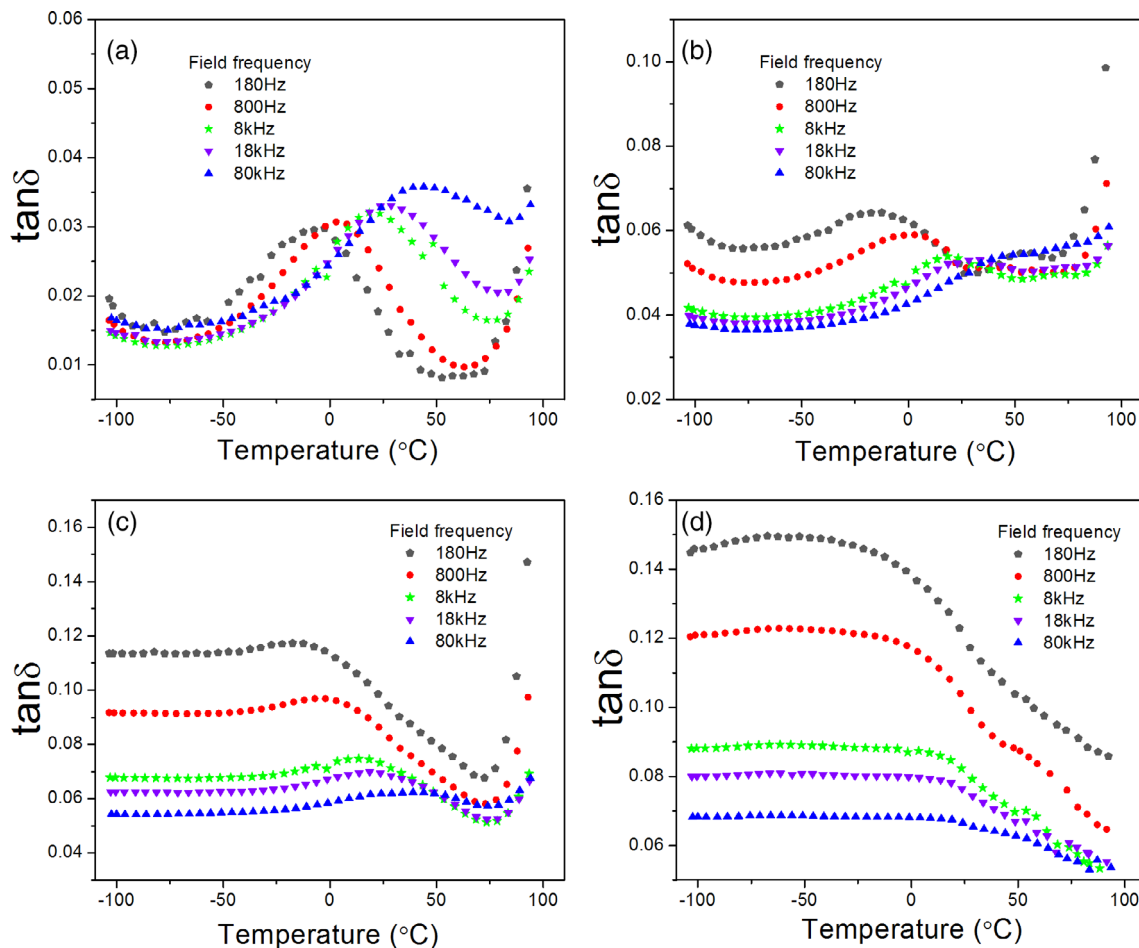


**FIGURE 7** Temperature dependence of  $\tan\delta$  at different frequencies (180 Hz, 800 Hz, 8 kHz, 18 kHz, 80 kHz) for (a) pure epoxy, (b) epoxy/GF6, (c) epoxy/GF10, and (d) epoxy/GF15 composites. [Color figure can be viewed at [wileyonlinelibrary.com](http://wileyonlinelibrary.com)]

prominent in the epoxy/GF15 composite with the highest loading content and is caused by failure of the interfacial polarization mechanism which cannot follow the applied field at higher frequencies.<sup>21,40</sup>

### 3.2.2 | Dielectric losses

The temperature dependence of the dielectric losses,  $\tan\delta$ , at different frequencies for pure epoxy and graphite flakes-loaded epoxy composites, are shown in the Figure 7a–d. The  $\tan\delta$  value increases with increasing frequency, as well as with the loading content, for each test frequency. The wide peak in  $\tan\delta$  versus  $T$  function which is clearly observable for pure epoxy matrix, as well as for epoxy/GF6 composite, is associated to the  $\beta$ -relaxations of the side groups of epoxy molecules. The position of that peak is shifted toward higher temperatures as the frequency increases, which is in accordance with the literature.<sup>11,39</sup> On the contrary, in the epoxy/GF10 and epoxy/GF15 composites, the  $\tan\delta$  value is

almost constant at low temperatures ( $T < -23^\circ\text{C}$  and  $T < -3^\circ\text{C}$ , for the epoxy/GF10 and epoxy/GF15, respectively), at all frequencies. Such behavior is caused by the Maxwell–Wagner polarization effect, that is, the accumulation of charge carriers at the graphite/epoxy interface. A wide peak, related to the  $\beta$ -relaxations, can be also noticed in composites loaded with 15 wt% of graphite flakes, especially at lower frequencies ( $<1$  kHz), but this peak seems screened with other processes.

For temperatures  $T > 75^\circ\text{C}$ , pronounced increase of  $\tan\delta(T)$  is observed in pure epoxy, epoxy/GF6, and epoxy/GF10 composites, but not in the epoxy/GF15. The observed increase can be due to the  $\alpha$ -relaxations (related to the rotation of segments of main polymer chains close and above the glass transition temperature,  $T_g$ ). Absence of the  $\tan\delta(T)$  increase in epoxy/GF15 can be explained by the fact that the spacing between particles of filler is greatly reduced in this composite, which reduces the possibility for rotation of the epoxy segments.

Figure 6b shows the frequency dependence of dielectric losses for composites loaded with 6, 10, and 15 wt%



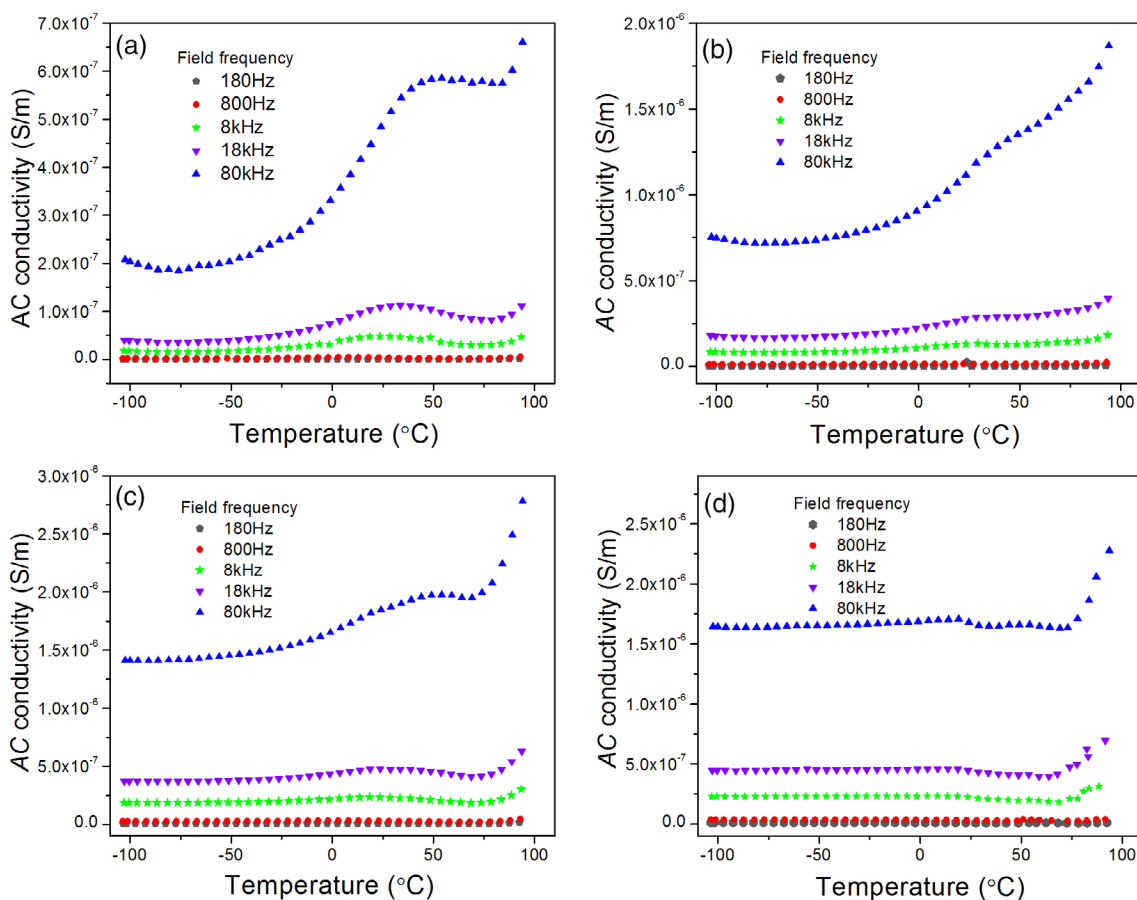


**FIGURE 8** Temperature dependence of *ac* conductivity at different test frequencies for (a) pure epoxy; (b) epoxy/GF6; (c) epoxy/GF10, and (d) epoxy/GF15. [Color figure can be viewed at [wileyonlinelibrary.com](http://wileyonlinelibrary.com)]

of GF, at  $T = 17^\circ\text{C}$ . Again, with increasing the loading, the dielectric losses increase, at all tested frequencies, while with increasing the frequency the dielectric losses decrease in the epoxy/GF15 and epoxy/GF10 composites (but less pronounced in the epoxy/GF10). In the epoxy/GF6 composite, the  $\tan\delta$  value changes insignificantly with increasing frequency, what is in accordance with the results published by Corcione et al.<sup>18</sup> Generally, at lower frequencies, various types of polarization are active (interfacial, dipolar, atomic, ionic, etc.), leading to a higher dielectric losses. At higher frequencies, many of the polarization mechanisms fade out which results in the  $\tan\delta$  decrease (here it could be due to the Maxwell–Wagner (MW) *interfacial* polarization fade out).

### 3.2.3 | AC conductivity

Temperature dependences of the *ac* conductivity,  $\sigma_{ac}$ , of pure epoxy and composites, measured at different frequencies (from 180 Hz to 80 kHz), are presented in the Figure 8a–d. As can be seen, the *ac* conductivity increases

with temperature increase, for pure epoxy and composites doped with 6 and 10 wt%. On the contrary, in the epoxy/GF15 composite the *ac* conductivity remains almost constant with increasing temperature up to ca.  $67^\circ\text{C}$ , for all frequencies, pointing out that there is no any thermally activated conduction mechanism in this composite.

Generally, electrical transport in polymer composites can occur either through direct contact between the conductive fillers or through the tunneling of electrons between the sufficiently close conductive particles. As a result, the *ac* conductivity of composites based on epoxy resin and the GF comes from: (i) *Ohmic conduction*, that is frequency independent and enabled by direct contact of graphite flakes, and (ii) *non-Ohmic conduction*, that is frequency dependent and occur through the barrier-tunneling effect between graphite flakes and an epoxy layer.

Figure 6c shows the frequency dependences of the *ac* conductivity of all three composites, at temperature  $17^\circ\text{C}$ . In the low-frequency region, the *ac* conductivity is practically independent on frequency, while in the high-

frequency region  $\sigma_{ac}$  strongly depends on  $f$ . In the frequency interval from 30 Hz to 140 kHz, the  $\sigma_{ac}$  values change from  $10^{-9}$  to  $10^{-6}$   $\text{Sm}^{-1}$ . The frequency dependence of the  $ac$  conductivity can give information about the conduction mechanism in composites. The frequency dependence of  $\sigma_{ac}$  generally follows the universal dynamic response, which can be described by *Jonscher* relation<sup>41</sup>:  $\sigma_{ac}(\omega) = \sigma_0 + A\omega^n$ , where  $\sigma_0$ —is the  $dc$  conductivity of the composite,  $A$ —is a constant which determines the strength of polarizability,  $n$ —is a power-law exponent ( $0 \leq n \leq 1$ ) that represents the degree of carriers' interactions with the lattice, and  $\omega = 2\pi f$ —is the angular frequency of the applied electric field. Our experimentally obtained  $\sigma_{ac}(f)$  plots were fitted using *Jonscher* relation. For the parameter  $n$  were obtained: 1, 0.95 and 0.887 value, for epoxy/GF6, epoxy/GF10, and epoxy/GF15 composites, respectively. As we can notice, the  $n$  value decreases with graphite concentration increase. In the literature, the value of  $n = 0.86$  was reported for composites close to the percolation threshold,  $p_c$  at which the insulating-conducting transition can be observed.<sup>5,42</sup>

Based on the above analysis of  $\sigma_{ac}(T)$  and  $\sigma_{ac}(f)$  plots, we can conclude that in the composites loaded with graphite flakes up to 10 wt% the dominant conduction mechanism is tunneling of electrons through the network of formed micro-capacitors, while in the epoxy/GF15 composite conduction is most likely achieved through direct contacts between fillers which enable free-charge migration.

According to Kranauskaite et al.,<sup>5</sup> for randomly dispersed, conducting graphite flakes in epoxy matrix, the expected percolation threshold,  $p_c$ , is inversely proportional to the aspect ratio,  $A$ , of graphite flakes, that is,  $p_c \sim 1/A$ , where  $A$  is defined as the ratio of lateral dimension to thickness of a flake particle. This relation is derived from the percolation theory, whose validity can be limited for high aspect ratio nanoparticles (e.g., carbon nanotubes, graphene, etc.).<sup>43</sup> Anyway, according to this approach, the expected  $p_c$  value for the flaky graphite filler with the aspect ratio  $A = 10$  lays inside the interval  $18 \text{ wt}\% \leq p_c \leq 26 \text{ wt}\%$ .<sup>5</sup> In order to estimate the aspect ratio of GF used in this work, we performed the measurements of the specific BET surface area,  $S_{\text{BET}}$ . Then, the average graphite flake thickness,  $L_c$  (in nm) was estimated using the formula:  $S_{\text{BET}} = 2630c/(2 L_c)$ , where  $2630 \text{ m}^2/\text{g}$  is the theoretical specific surface of a single graphene layer and  $c = 0.67 \text{ nm}$  is the graphite lattice parameter along the  $z$  axis.<sup>44</sup> Experimentally obtained  $S_{\text{BET}}(\text{GF}) = 39.8 \text{ m}^2/\text{g}$  value yields the estimated GF flakes thickness of 22 nm. If we assume that the lateral dimension of GF is  $\sim 1 \mu\text{m}$  (see Figure 1), the expected aspect ratio,  $A$  is  $>45$ , but  $A$  could be much higher ( $>200$ ), if the lateral size of graphite flakes is  $\sim 10 \mu\text{m}$ .

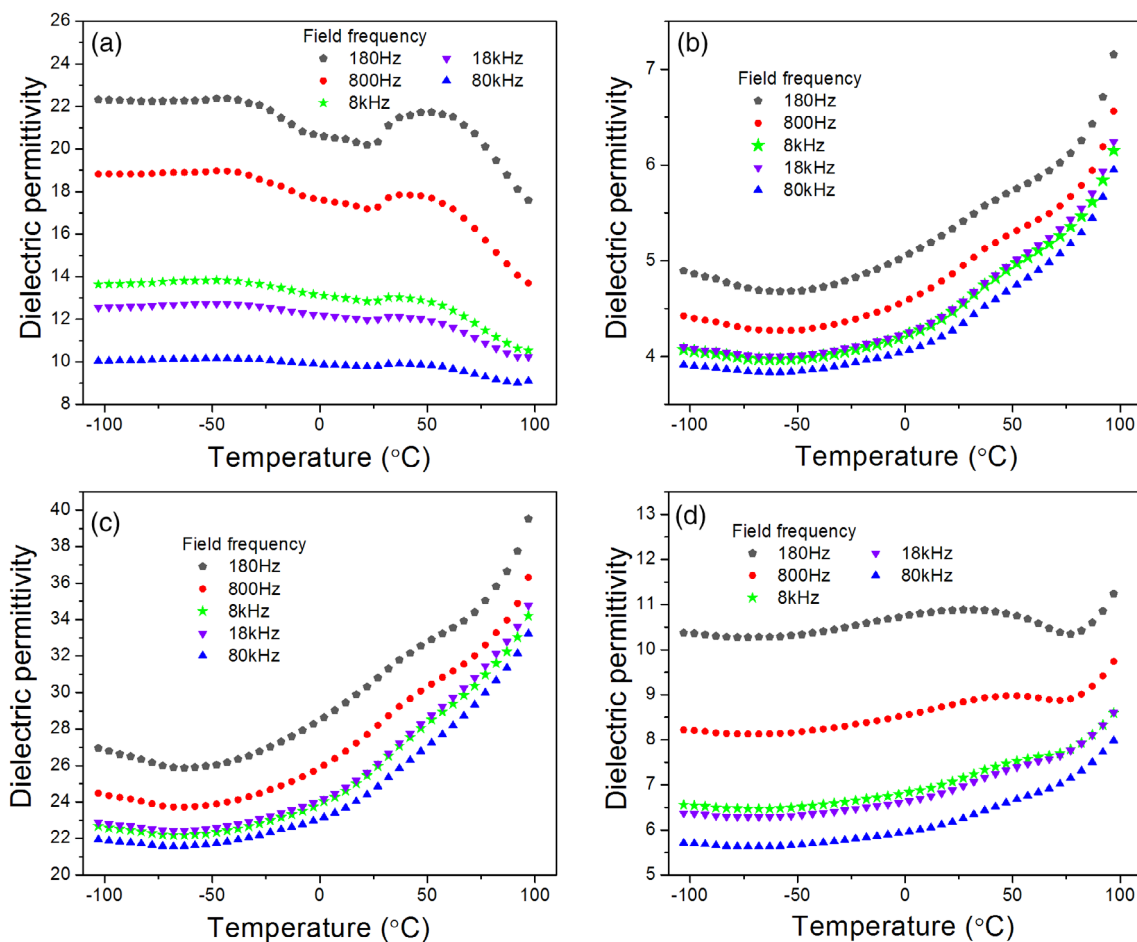
Thus, it is most probable that in the epoxy/GF15 composite process of free-charge migration via network of GF flakes in direct contact occurs.

### 3.3 | The effect of surface functionalization on dielectric properties of composites loaded with 5 wt% of graphite flakes

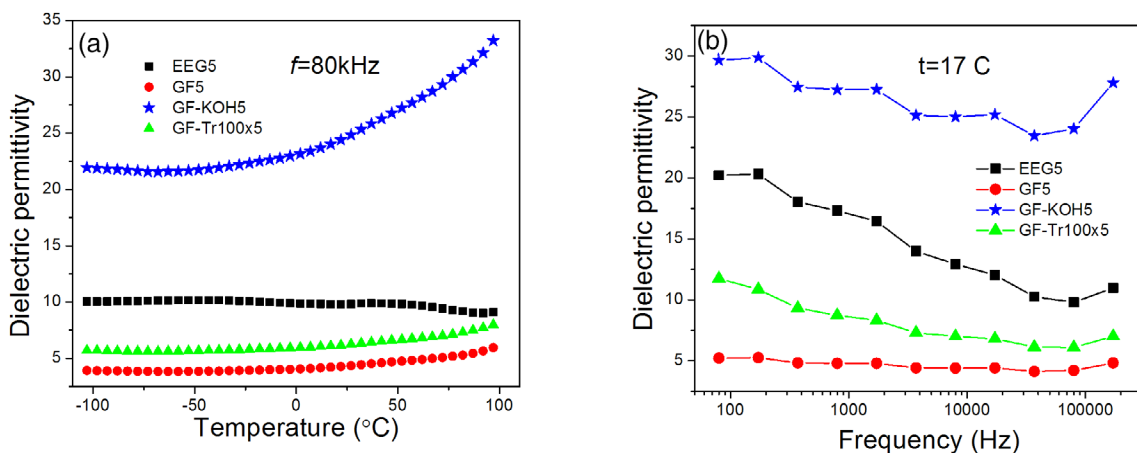
Dielectric properties of composites are not influenced only by the amount of added filler in a polymer matrix, but also depend on the filler geometry (shape, the lateral size, the aspect ratio), filler surface chemistry and inherent conductivity, as well as on the nature of the filler/matrix interface. In order to study the effect of the filler surface chemistry on dielectric properties, four different composites loaded with 5 wt% graphite flakes were prepared. Beside the epoxy/GF5 composite, we prepared the composites loaded with graphite flakes whose surface was treated with KOH (epoxy/GF-KOH5) or with Triton-100x (epoxy/GF-Tr100x5), as explained in the section 2.1. For the sake of comparison, we have also studied behavior of the epoxy/EEG5 sample, loaded with EEG flakes obtained by prolonged sonication of exfoliated expanded graphite.<sup>19</sup> EEG flakes have significantly higher aspect ratio as compared to GF flakes (Figure 1).

Figure 9a–d shows the temperature dependence of dielectric permittivity,  $\epsilon_r(T)$ , for epoxy/EEG5, epoxy/GF5, epoxy/GF-KOH5, and epoxy/GF-Tr100x5 composites, measured at 180 Hz, 800 Hz, 8 kHz, 18 kHz, and 80 kHz. Two samples, the epoxy/GF5 and epoxy/GF-KOH5 show similar  $\epsilon_r(T)$  behavior resembling that of the epoxy/GF6 composite (see Figure 5b). On the contrary, the  $\epsilon_r(T)$  dependence of the epoxy/EEG5 and epoxy/GF-Tr100x5 composites show significantly different features. Such a behavior can be caused by a different filler geometry and surface chemistry, as compared to the GF and GF-KOH flakes. The ATR-FTIR spectra of GF flakes (Figure 2c) revealed the absence of functional groups on the surface of graphite layers. Dry milling with potassium hydroxide, KOH, inevitably increases the number of oxygen-containing groups (carbonyl [C=O], carboxyl [—COOH] and hydroxyl [—OH]),<sup>31</sup> as well as defect sites inside  $\text{sp}^2$  graphite layer (Figure 2c). On the contrary, functionalization with Triton-100x hosts polyethylene oxide chains on a surface of GF flakes, whose polarization in an electric field influence the dielectric response.

It is worth noticing that the epoxy/GF-KOH5 has the highest dielectric permittivity at all measured temperatures, regardless the frequency (see Figure 9a–d). This fact is also confirmed by recording the  $\epsilon_r(T)$  dependence at fixed low frequency value of 80 kHz (Figure 10a).



**FIGURE 9** Temperature dependence of dielectric permittivity for (a) epoxy/EEG5, (b) epoxy/GF5, (c) epoxy/GF-KOH5, and (d) epoxy/GF-Tr100x5 composites, at 180 Hz, 800 Hz, 8 kHz, 18 kHz, and 80 kHz. [Color figure can be viewed at [wileyonlinelibrary.com](http://wileyonlinelibrary.com)]



**FIGURE 10** Variation of dielectric permittivity (a) with temperature, at 80 kHz and (b) with frequency, at 17°C, for epoxy/EEG5, epoxy/GF5, epoxy/GF-KOH5, and epoxy/GF-Tr100x5 composites. [Color figure can be viewed at [wileyonlinelibrary.com](http://wileyonlinelibrary.com)]

There are several possible explanations for such a behavior. On one hand, the surface of GF-KOH flakes is rich with —OH groups (see Figure 2c) which can serve as adsorption sites for the molecular water from environment.<sup>7,45</sup>

These polar water molecules serve further as an additional dipolar polarization source responsible for the increase of dielectric permittivity. Also, a better compatibility between GF-KOH flakes and epoxy resin can be

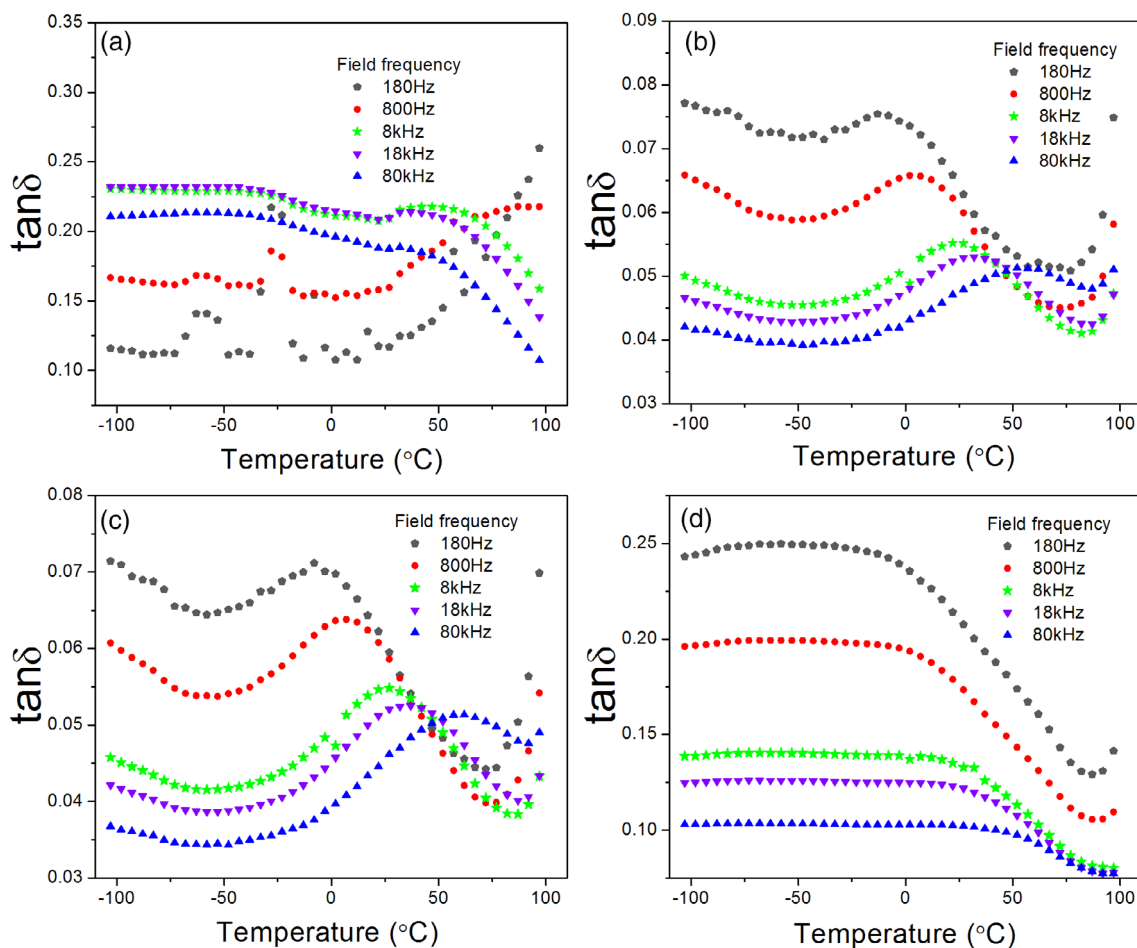


**FIGURE 11** Temperature dependence of  $\tan\delta$  at different frequencies (180 Hz, 800 Hz, 8 kHz, 18 kHz, 80 kHz) for (a) epoxy/EEG5, (b) epoxy/GF5, (c) epoxy/GF-KOH5, and (d) epoxy/GF-Tr100x5 composites. [Color figure can be viewed at [wileyonlinelibrary.com](https://onlinelibrary.wiley.com/doi/10.1002/app.54881)]

expected.<sup>18</sup> Yet, we cannot exclude the presence of the so-called “graphite dust” (smaller graphite particles), observed by SEM (Figure 1d), whose presence between graphite flakes separated by an epoxy can potentially change capacity of the nanoscale capacitors.<sup>6</sup> In addition, composites obtained with GF and GF-KOH flakes show a prominent increase of the  $\epsilon_r$  value at temperatures  $T > 7^\circ\text{C}$ , what is not characteristic for epoxy/EEG5 and epoxy/GF-Tr100x5. This is probably due to a higher aspect ratio of EEG, direct contact between EEG occurs with 5 wt% of loading.<sup>19</sup> This enable free electron migration and consequently different dielectric response of epoxy/EEG5 composite (Figure 9a). At  $17^\circ\text{C}$ , the measured dielectric permittivity slightly decreases with the electric field frequency,  $f$ , increase up to the approximately 80 kHz (Figure 10b).

The temperature dependences of dielectric losses,  $\tan\delta$ , further indicate the similarity between the composites filled with EEG and GF-Tr100x (Figure 11). For the same loading rate of 5 wt%, the dielectric losses of epoxy composites filled with EEG or GF-Tr100x follow the

similar dependence on temperature and have similar values, being approximately three times higher than the  $\tan\delta$  of the epoxy/GF5 and epoxy/GF-KOH5 at low temperatures and frequency. One can also note that the temperature dependence of  $\tan\delta$  of epoxy/GF5 and epoxy/GF-KOH5 at different frequencies is very similar to the behavior of the epoxy/GF6 (Figure 6b).

It is interesting to note that the surface treatment with KOH notably increased the dielectric constant of the epoxy/GF-KOH5 composite, without changing the dielectric loss relative to the counterpart, the epoxy/GF5 composite. On the contrary, the surface treatment with Triton-100x significantly increased the dielectric loss of the epoxy/GF-Tr100x5 composite in a way that it became comparable to the dielectric losses of the epoxy/EEG5. It is known that for EEG flakes it is easier to form a conductive path due to the higher aspect ratio as compared to the GF flakes. Therefore, the dielectric losses increased as a consequence of better conductivity and leakage current occurrence.<sup>46</sup>

The temperature dependence of  $ac$  conductivity of these four composites (loaded with 5 wt% of different

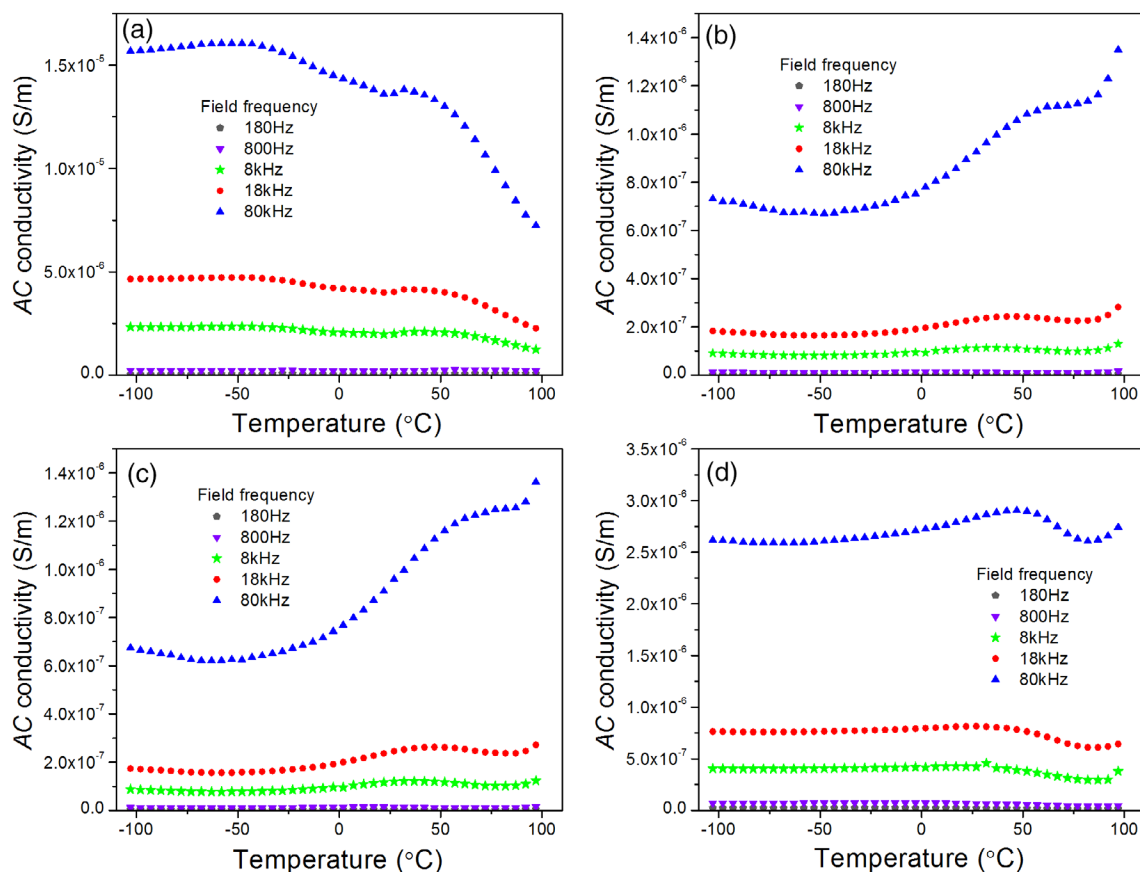


**FIGURE 12** Temperature dependence of AC conductivity for different frequencies (180 Hz, 800 Hz, 8 kHz, 18 kHz, 80 kHz) for (a) epoxy/EEG5, (b) epoxy/GF5, (c) epoxy/GF-KOH5, and (d) epoxy/GF-Tr100x5 composites. [Color figure can be viewed at [wileyonlinelibrary.com](https://onlinelibrary.wiley.com/terms-and-conditions)]

graphite fillers), measured at frequencies 180 Hz, 800 Hz, 8 kHz, 18 kHz, and 80 kHz are shown on Figure 12. Three composites loaded with GF flakes follow similar temperature dependence for all frequencies, while the behavior of the composite made with EEG flakes differs and strongly depends on the electric field frequency value. The  $\sigma_{ac}$  conductivity of this composite is for one order of magnitude higher than the  $\sigma_{ac}$  of composites obtained when GF, GF-KOH, and GF-Tr100x flakes were used. Since, the EEG flakes have much higher aspect ratio than the GF, it is easier to establish the conducting network applying lower loading content of EEG (i.e.,  $p_c \sim 3$  wt%).<sup>19</sup> At the same time, inherent conductivity of exfoliated expanded graphite flakes, EEG, can differ from those of GF flakes due to a lower density of defects inside  $sp^2$ -planes in EEG, comparing to GF.

#### 4 | CONCLUSIONS

In summary, dielectric properties of composites based on epoxy matrix loaded with different content (5–15 wt%) of

GF have been analyzed. Dielectric permittivity ( $\epsilon_r$ ), dielectric loss ( $\tan\delta$ ), and  $ac$  conductivity ( $\sigma_{ac}$ ) of the composites have been determined in wide temperature (−103 to 97°C) and frequency (20 Hz–200 kHz) range. The results show that with increasing concentration of GF filler, values of dielectric permittivity  $\epsilon_r$  increased regardless of the temperature, at every test frequency. In composites loaded with GF flakes up to 10 wt%, the dominant conduction mechanism is tunneling of electrons, while loading of 15 wt% gives rise to the electron conduction through direct contacts between fillers. For composites with constant loading content of 5 wt%, dielectric properties have been changed depending on the filler surface chemistry and geometry. Thus, using the GF obtained upon dry milling in the presence of KOH, notably increase dielectric constant of the epoxy/GF-KOH5 composite, without changing dielectric losses relative to the counterpart, the epoxy/GF5 composite. Such behavior can be due to (i) the GF-KOH surface enriched with —OH groups and polar water molecules; (ii) a better compatibility between GF-KOH flakes and epoxy resin and (iii) the presence of “graphite dust.” On the contrary, the

surface treatment with Triton-100x significantly increased dielectric loss of the composite in a way that became comparable to the dielectric losses of the one loaded with exfoliated expanded graphite. In addition, the epoxy/EEG5 composite shows higher *ac* conductivity than those obtained with flaky graphite, GF. In conclusion, the best results in terms of conductivity are seen for the epoxy/EEG5 composite, while the highest dielectric permittivity values, of the four studied samples loaded with 5 wt% fillers, has the epoxy/GF-KOH5 composite. The obtained results can provide new ways to design composites having specific dielectric properties.

## AUTHOR CONTRIBUTIONS

**Slavica Maletić:** Formal analysis (lead); investigation (lead); writing – review and editing (lead). **Nataša Jović Orsini:** Formal analysis (lead); investigation (lead); writing – review and editing (lead). **Mirjana Milić:** Formal analysis (equal); writing – review and editing (equal). **Jablan Dojčilović:** Formal analysis (supporting); writing – review and editing (supporting). **Amelia Montone:** Formal analysis (equal); writing – review and editing (equal).

## ACKNOWLEDGMENTS

This work was supported by the Ministry of Science, Technology Development and Innovations of the Republic of Serbia (contract nos. 451-03-47/2023-01/200017 and 451-03-47/2023-01/200162). The authors acknowledge the assistance and support of Dr. Carlo Alvani and Dr. Gianfranco Carotenuto for  $S_{\text{BET}}$  and MAS measurements, respectively.

## CONFLICT OF INTEREST STATEMENT

The authors declare no conflict of interest.

## DATA AVAILABILITY STATEMENT


The data will be available from the corresponding author upon reasonable request.

## ORCID

Slavica Maletić  <https://orcid.org/0000-0001-8516-7245>

Nataša Jović Orsini  <https://orcid.org/0000-0003-1613-3361>

Mirjana Milić  <https://orcid.org/0000-0002-0285-2819>

Jablan Dojčilović  <https://orcid.org/0000-0002-8391-9842>

Amelia Montone  <https://orcid.org/0000-0002-1570-3644>

## REFERENCES

- [1] A. Osman, A. Elhakeem, S. Kaytbay, A. Ahmed, *Adv. Compos. Hybrid. Mater.* **2022**, *5*, 547.

- [2] A. J. Marsden, D. G. Papageorgiou, C. Vallés, A. Liscio, V. Palermo, M. A. Bissett, R. J. Young, I. A. Kinloch, *2D Mater.* **2018**, *5*, 032003.
- [3] W. Zhang, A. A. Dehghani-Saniij, R. S. Blackburn, *J. Mater. Sci.* **2007**, *42*, 3408.
- [4] S. Ruiz, J. A. Tamayo, J. Delgado Ospina, D. P. Navia Porras, M. E. Valencia Zapata, J. H. Mina Hernandez, C. H. Valencia, F. Zuluaga, C. D. Grande Tovar, *Biomolecules* **2019**, *9*, 109.
- [5] I. Kranauskaite, J. Macutkevicius, P. Kuzhir, N. Volynets, A. Paddubskaya, D. Bychanok, S. Maksimenko, J. Banys, R. Juskenas, S. Bistarelli, A. Cataldo, F. Micciulla, S. Bellucci, V. Fierro, A. Celzard, *Phys. Status Solidi A* **2014**, *211*, 1623.
- [6] N. Yousefi, X. Sun, X. Lin, X. Shen, J. Jia, B. Zhang, B. Tang, M. Chan, J. K. Kim, *Adv. Mater.* **2014**, *26*, 5480.
- [7] M. Qin, L. Zhang, H. Wu, *Adv. Sci.* **2022**, *9*, 2105553.
- [8] Y. Chekanov, R. Ohnogi, S. Asai, M. Sumita, *J. Mater. Sci.* **1999**, *34*, 5589.
- [9] Y. Poplavko, *Dielectric Spectroscopy of Electronic Materials: Applied Physics of Dielectrics*, Woodhead Publishing, Cambridge **2021**.
- [10] D. I. Bower, *An Introduction to Polymer Physics*, Cambridge University Press, Cambridge **2002**.
- [11] F. Kremer, A. Schönhal, *Broadband Dielectric Spectroscopy*, Springer Berlin, Heidelberg **2002**.
- [12] H. Fröhlich, *Theory of Dielectrics: Dielectric Constant and Dielectric Loss*, 2nd ed., Oxford at the Clarendon Press, Oxford **1987**.
- [13] H. Jdidi, N. Fourati, C. Zerrouki, L. Ibos, M. Fois, A. Guinault, W. Jilani, S. Guermazi, H. Guermazi, H. Guermazi, *Polymer* **2021**, *228*, 123882.
- [14] Y. P. Mamunya, Y. V. Muzychenko, P. Pissis, E. V. Lebedev, M. I. Shut, *Polymer. Eng. Sci.* **2002**, *42*, 90.
- [15] N. K. Srivastava, V. K. Sachdev, R. M. Mehra, *J. Polym. Sci.* **2007**, *104*, 2027.
- [16] T. Van Khai, G. N. Han, D. S. Kwak, Y. J. Kwon, H. Ham, K. B. Shim, H. W. Kim, *J. Mater. Chem.* **2012**, *22*, 17992.
- [17] C. Min, D. Yu, J. Cao, *Carbon* **2013**, *55*, 116.
- [18] C. Esposito Corcione, A. Maffezzoli, *Polym. Test.* **2013**, *32*, 880.
- [19] N. Jović, D. Dudić, A. Montone, M. Vittori Antisari, M. Mitrčić, V. Djoković, *Scripta Mater.* **2008**, *58*, 846.
- [20] N. Chand, D. Jain, *Bull. Mater. Sci.* **2004**, *27*, 227.
- [21] C. Chen, Y. Gu, S. Wang, Z. Zhang, M. Li, Z. Zhang, *Compos. Part. A: Appl. Sci.* **2017**, *94*, 199.
- [22] L. L. Vovchenko, O. V. Lozitsky, V. V. Oliynyk, V. V. Zagorodnii, T. A. Len, L. Y. Matzui, Y. S. Milovanov, *Appl. Nanosci.* **2020**, *10*, 4781.
- [23] C. Hu, H. Zhang, N. Neate, M. Fay, X. Hou, D. Grant, F. Xu, *Polymer* **2022**, *14*, 2583.
- [24] M. L. Sham, J. K. Kim, *Carbon* **2006**, *44*, 768.
- [25] N. A. Kotov, *Nature* **2006**, *442*, 254.
- [26] X. Zhang, G. Liang, J. Chang, A. Gu, L. Yuan, W. Zhang, *Carbon* **2012**, *50*, 4995.
- [27] T. Wang, X. Hu, X. Qu, S. Dong, *J. Phys. Chem. B* **2006**, *110*, 6631.
- [28] W. Genetti, W. L. Yuan, B. P. Grady, E. A. O'rear, C. L. Lai, D. T. Glatzhofer, *J. Mater. Sci.* **1998**, *33*, 3085.
- [29] J. Lin, J. Zhou, M. Guo, D. Chen, G. Chen, *Polymer* **2020**, *14*, 3660.
- [30] D. Fattakhova Rohlfing, A. Kuhn, *Carbon* **2006**, *44*, 1942.

- [31] H. Pan, L. Liu, Z. X. Guo, L. Dai, F. Zhang, D. Zhu, R. Czerw, D. L. Carroll, *Nano Lett.* **2003**, *3*, 29.
- [32] P. Mehra, C. Singh, I. Cherian, A. Giri, A. Paul, *ACS Appl. Energy Mater.* **2021**, *4*, 4416.
- [33] S. Wu, R. B. Ladani, J. Zhang, E. Bafekrpour, K. Ghorbani, A. P. Mouritz, C. H. Wang, *Carbon* **2015**, *94*, 607.
- [34] S. B. Maletic, D. D. Cerovic, J. R. Dojcilovic, *Nucl. Instrum. Methods Phys Res B* **2019**, *441*, 1.
- [35] D. D. Cerovic, K. A. Asanovic, S. B. Maletic, F. S. Marinkovic, I. M. Petronijevic, J. R. Dojcilovic, *J. Appl. Polym. Sci.* **2020**, *137*, 48456.
- [36] D. Vuković, B. Škipina, S. Maletić, D. D. Cerović, M.-M. Duvenhage, A. S. Luyt, D. Mirjanić, D. Dudić, *J. Appl. Polym. Sci.* **2021**, *138*, 50992.
- [37] A. S. Mazur, M. A. Vovk, P. M. Tolstoy, *Fuller. Nanotub. Carbon Nanostruct* **2020**, *28*, 202.
- [38] Y. Si, E. T. Samulski, *Nano Lett.* **2008**, *8*, 1679.
- [39] S. L. Wu, I. C. Tung, *J. Polym. Comp.* **1995**, *16*, 233.
- [40] T. K. Bindu Sharmila, J. V. Antony, M. P. Jayakrishnan, P. M. Sabura Beegum, E. T. Thachil, *Mater Des* **2016**, *90*, 66.
- [41] A. K. Jonscher, *J. Phys. D: Appl. Phys.* **1999**, *32*, R57.
- [42] Y. Song, T. W. Noh, S. I. Lee, J. R. Gaines, *Phys. Rev. B* **1986**, *33*, 904.
- [43] M. H. G. Wichmann, J. Sumfleth, B. Fiedler, F. H. Gojny, K. Schulte, *Mech. Compos. Mater.* **2006**, *42*, 395.
- [44] A. Peigney, C. Laurent, E. Flahaut, R. R. Bacsa, A. Rousset, *Carbon* **2001**, *39*, 507.
- [45] R. Zafar, N. Gupta, *IET Nanodielectrics* **2020**, *3*, 20.
- [46] C. L. Poh, M. Mariatti, A. F. M. Noor, O. Sidek, T. P. Chuah, S. C. Chow, *Compos. Part B: Eng.* **2016**, *85*, 50.

**How to cite this article:** S. Maletić, N. Jović Orsini, M. Milić, J. Dojcilović, A. Montone, *J. Appl. Polym. Sci.* **2023**, e54881. <https://doi.org/10.1002/app.54881>